

Non-resonant gas
bubbles in sound
backscattering
and attenuation in
the sea*

OCEANOLOGIA, No. 31
pp. 87-95, 1991.
PL ISSN 0078-3234

Marine acoustics
Gas bubbles
Backscattering
Attenuation

JOANNA SZCZUCKA
Institute of Oceanology,
Polish Academy of Sciences,
Sopot

W. Pomorskiej 55

Manuscript received June 14, 1991, in final form October 7, 1991.

Abstract

Backscattering and absorption of sound energy by gas bubbles in the sea are dominated by bubbles of the resonant size, so the experimental determination of bubble concentration in the sea is based on the resonance approximation. The resonance algorithm was reexamined in order to find the reasons for the visible discrepancies between the bubble size spectra obtained by optical and acoustic methods (in particular in the small radii area). Some theoretical distributions were chosen and compared with the distributions inferred from the resonant calculations. It was shown that using very high insonifying frequencies to estimate the density of very small bubbles can lead to a significant overestimation of the bubble population.

1. Introduction

Gas bubble concentration in sea surface waters is one of the most important factors in the processes of gas exchange between the sea and the atmosphere. It is measured *in situ* by acoustic or optical methods (see References) and the formula describing the dependence of bubble density on the bubble size and on the depth of their occurrence is deduced. Such a formula is necessary for the mathematical modelling of numerous marine processes involving gas bubbles (aerosol production, raising suspensions and bacteria from the deep layers to the surface) as well as for modelling of sound propagation conditions in the sea with gas bubbles. The results of our own measurements are compared with other *in situ* both acoustic and optical

* The investigations were carried out as part of the research programme CPBP 03.10, co-ordinated by the Institute of Oceanology of the Polish Academy of Sciences.

experiments in Figure 1. Despite the significant differences in the absolute values of bubble densities (they are the consequence of different regions, seasons and, possibly, different generation mechanisms), there is a visible discrepancy in the character of the bubble size spectrum obtained by optical (Johnson and Cooke, 1979; Kolobayev, 1975) and acoustic methods (Akulichev *et al.*, 1986; Lovik, 1980; Medwin, 1970; Szczucka, 1990). In the small radii domain there are distinct maxima in the 'optical' distributions and no maxima in the 'acoustic' ones. These differences are thought to be caused by such factors as the limited resolution of optical measurements, assuming other strange objects to be bubbles, or neglecting the viscoelastic phenomena in acoustic methods. The physical formalism of the acoustic resonance-based experimental methods has been revised, but attempts to correct the previously obtained distributions have yielded no significant results (MacIntyre, 1986).

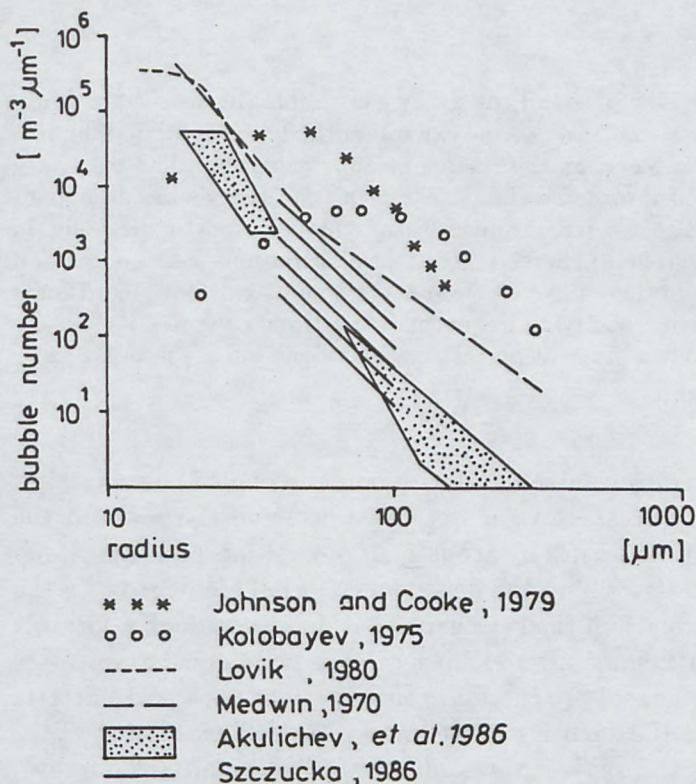


Fig. 1. Bubble size spectra from different experiments

The aim of this paper is to re-examine the applicability of the resonance algorithm and to estimate the nonresonant contribution in the processes of sound energy scattering and attenuation by gas bubbles in the sea.

2. Theory – a brief review

The relationship between the radius of an air bubble and its resonant frequency is expressed by

$$f_R[\text{kHz}] = \frac{3280\sqrt{1 + 0.1z}}{a[\mu\text{m}]}, \quad (1)$$

and the scattering and extinction cross-section of an individual bubble are given by

$$\sigma_s = \frac{4\pi a^2}{\left(\frac{f^2}{f_R^2} - 1\right)^2 + \delta^2}, \quad (2)$$

$$\sigma_e = \frac{4\pi a^2 \frac{\delta}{\delta_r}}{\left(\frac{f^2}{f_R^2} - 1\right)^2 + \delta^2}, \quad (3)$$

where

a – bubble radius,

δ – total damping constant (due to reradiation, thermal and viscosity effects),

δ_r – damping constant due to reradiation only,

f – incident sound frequency,

f_R – resonant frequency.

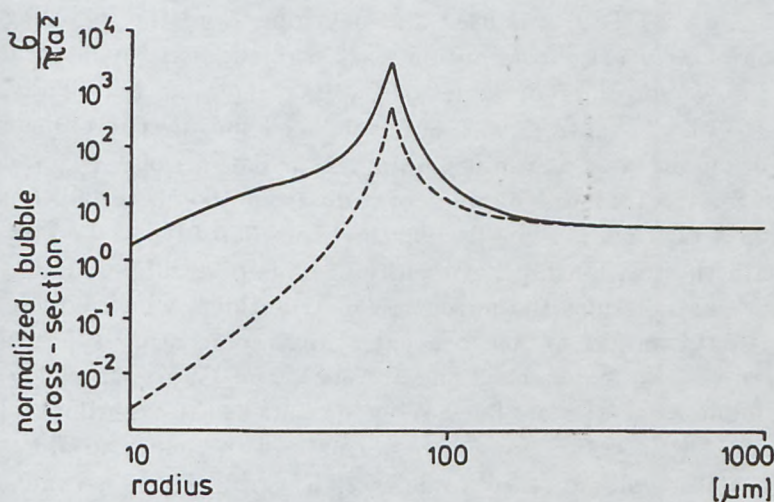


Fig. 2. Normalized single bubble cross-sections for scattering (dashed line) and extinction (solid line) versus bubble radii for sound frequency 50 kHz

These dependences are shown in Figure 2. It can be seen that σ_s and σ_e have sharp maxima at resonance frequencies; their resonant values are

hundreds of times greater than the geometrical cross-section of the bubble. The cross-sections per unit volume in a population of noninteracting bubbles of diverse radii are obtained by integrating individual size terms

$$S_s(f) = \int_0^{\infty} n(a)\sigma_s(a, f)da, \quad (4)$$

$$S_e(f) = \int_0^{\infty} n(a)\sigma_e(a, f)da. \quad (5)$$

The assumption of the dominant role of the resonant elements (Szczucka, 1986) leads to the expressions

$$S_s = \frac{2\pi^2 a_R^3 n(a_R)}{\delta_R}, \quad (6)$$

$$S_e = \frac{2\pi^2 a_R^3 n(a_R)}{\delta_{rR}}. \quad (7)$$

So, using a sound beam with a fixed frequency, the resonant values of radius a_R and damping δ_R and δ_{rR} are calculated, and on the basis of the measurement of scattering or extinction strength the resonant bubble concentration $n(a_R)$ is determined.

3. Numerical test

In order to check the sensitivity of the resonant algorithm, the idea of Commander and Moritz (1989) was used and developed and the following test carried out: an *a priori* size distribution was assumed, next the integral expressions (4) and (5) for different values of f were calculated, and finally, on the basis of (6) and (7), $n(a_R)$ was again deduced for the comparison with the distribution assumed at the beginning. Calculations of $S_s(f)$ and $S_e(f)$ were done for the resonant bubbles of radii from 10 μm to 300 μm occurring at a depth of 2 m, *i.e.* for frequencies from 360 kHz to 12 kHz, in accordance with the relationship between the radius of a bubble and its resonant frequency (1). Besides the power law distributions, which best fit the experimental data on gas bubble concentrations, some other types of distributions were tested: exponential (monotonic), and Gauss, Rayleigh, χ^2 , Cauchy and log-normal (the last five having maxima as the experimental 'optical' spectra). All these functions were normalized to yield a total gas volume per unit water volume (the 'void fraction') of $3 \cdot 10^{-7}$, as under natural conditions. Introductory computations showed the strong influence of the assumed integration limits on the results, so a suitably large interval of bubble radii was chosen [1.450 μm] to cover practically the whole spectrum of natural sea bubbles. Calculations were carried out for various distribution parameters, but because of the similarity of the results, only some of them

Table 1. Statistical distributions and their parameters used in the numerical test

Distribution		C	a_{\max}
Gauss	$a_0 = 60$		
$C \exp \left\{ -\frac{(a-a_0)^2}{2\sigma^2} \right\}$,	$\sigma = 30$	2519	60
Rayleigh			
$C \frac{a}{\sigma} \exp \left\{ -\frac{a^2}{2\sigma^2} \right\}$,	$\sigma = 50$	3048	50
χ^2	$\gamma = 0.1$		
$C(\gamma a)^{\lambda-1} \exp(-\frac{1}{2}\gamma a)$,	$\lambda = 2$	78	60
exponential			
$C \exp \left\{ -\frac{a}{k} \right\}$,	$k = 60$	979	-
Cauchy	$h = 10$		
$C \frac{h}{h^2 - (a-a_0)^2}$,	$a_0 = 60$	30625	60
log-normal	$a_0 = 60$		
$C \frac{1}{a} \exp \left\{ -\frac{\log a - \log a_0}{2\sigma^2} \right\}$,	$\sigma = 0.3$	27914	37.2
power law			
$C a^{-\beta}$	$\beta = 1$	$2.35 \cdot 10^3$	-
	$\beta = 2$	$7.06 \cdot 10^5$	-
	$\beta = 3$	$1.59 \cdot 10^8$	-
	$\beta = 4$	$1.07 \cdot 10^{10}$	-
	$\beta = 5$	$4.36 \cdot 10^{10}$	-
	$\beta = 6$	$5.96 \cdot 10^{10}$	-

were chosen for the analysis. Table 1 presents these distributions and their parameters.

Figure 3 and 4 show the distributions assumed *a priori* in comparison with those inferred from the resonance scattering and attenuation. In the $60 \mu\text{m} < a < 120 \mu\text{m}$ interval there is very good agreement between all three curves. However, for small radii ($a < 50 \mu\text{m}$) a divergence occurs, especially for scattering-based results. The extinction approximation gives slightly smaller errors in this region. The reverse situation takes place in the large radii domain, *i.e.* for small insonifying frequencies, where the scattering approximation seems to be good enough, but the attenuation approach produces significant errors (they are, however, less than the scattering-based errors in the small radii region). Power law distributions (Fig. 4) give much better results, especially in the resonance scattering approximation.

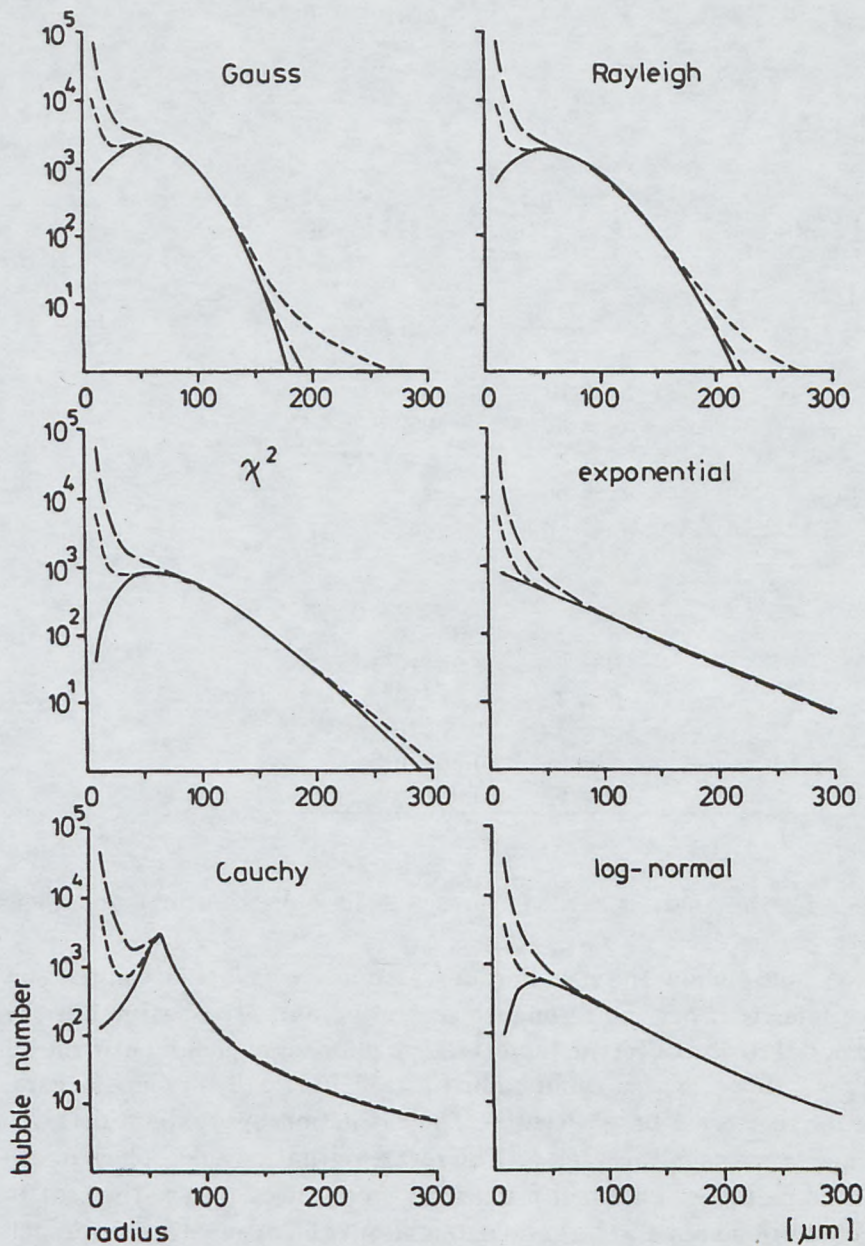


Fig. 3. Non-power law distributions of gas bubble concentrations assumed *a priori* (solid lines) and inferred from resonance scattering (long dashed lines) or from resonance attenuation theory (short dashed lines)

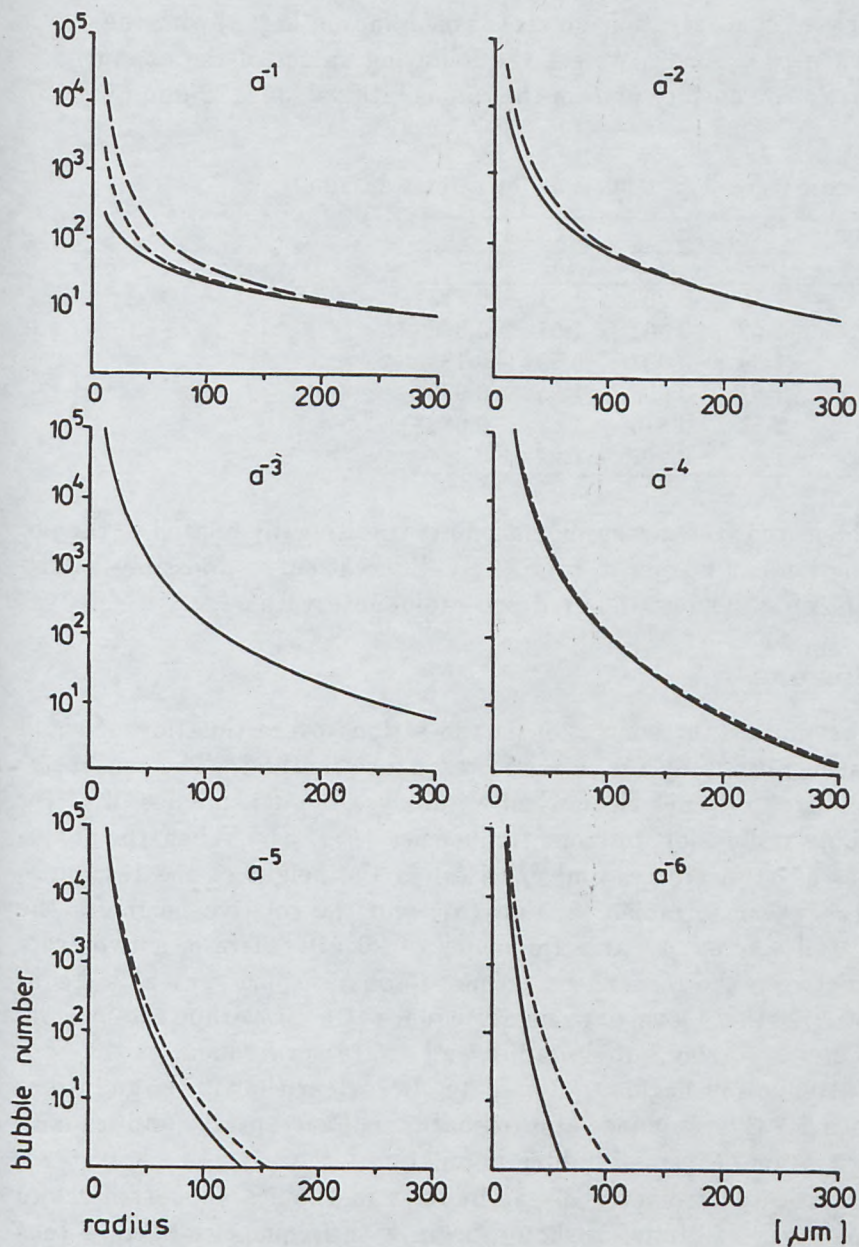


Fig. 4. Power law distributions of gas bubble concentrations assumed *a priori* (solid lines) and inferred from resonance scattering (long dashed lines) or from resonance attenuation theory (short dashed lines)

As we can see in Figure 1, the acoustic resonance measurements usually yield a limited bubble size spectrum due to the limited choice of possible sounding frequencies. This fact can explain the surprisingly good fit of the power law function to the results. If, for example, one tries to describe the resonance-based concentration curves (dashed lines in Fig. 3) with the power law function $n(a) = Aa^{-B}$, we get the following values of the exponent B and the correlation coefficient R in the radius interval [30, 120 μm] (Tab. 2):

Table 2. Linear regression coefficients for various distributions

Distribution	Scattering		Attenuation	
	B	R	B	R
Gauss	-1.72	-0.992	-1.11	-0.753
Rayleigh	-1.62	-0.961	-1.07	-0.868
χ^2	-1.34	-0.983	-0.59	-0.785
exponential	-1.81	-0.999	-1.25	-0.993
Cauchy	-2.51	-0.873	-1.67	-0.682
log-normal	-1.81	-0.997	-1.22	-0.967

It is evident that the measurement points traditionally related to the power law function can belong to completely different curves, possibly having a maximum (often beyond the analysed radius interval).

4. Conclusions

The most important conclusion is the serious overestimation of small bubble concentrations by the acoustic resonance method. The reason for this phenomenon becomes clear when we analyse the dependence of σ_s (or σ_e) on bubble radius for different frequencies (Fig. 5). When the frequency increases, a_R decreases and δ_R rises, so the height of the resonance peak decreases (see formulae (2) and (3)) and the relative height of the 'resonance tail' increases: at a frequency of 20 kHz there is a two-order difference between the resonance and non-resonance part, but at a frequency of 150 kHz these levels are nearly equal (at least within the interval of all naturally occurring bubble radii), and at greater frequencies the non-resonance attenuation begins to dominate. It is clear that for large insonifying frequencies the resonance approximation is unacceptable and leads to the overestimation of a small bubble population.

The acoustic spectrometry of gas bubbles in the sea should therefore be performed very carefully. It should begin with frequencies of some tens of kilohertz – where the resonance approximation is applicable – and after evaluating the concentration of bubbles of related size, larger and smaller frequencies can be used with a simultaneous correction for the contributions

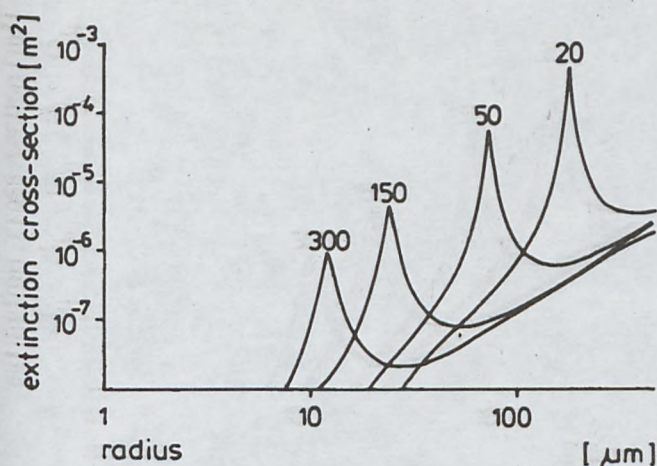


Fig. 5. Extinction cross-section of an individual bubble at several sound frequencies (f value in kHz marked over the resonance peak)

from the previously measured bubbles, which are non-resonant at those frequencies.

References

- Akulichev V. A., Bulanov V. A., Klenin S. S., 1986, *Akusticheskoye zondirovaniye gazovykh puzyrkov v morskoy srede*, Akust. Zh., 32, 3, 289–295.
- Commander K., Moritz E., 1989, *Off-resonance contributions to acoustical bubble spectra*, J. Acoust. Soc. Am., 85(6), 2665–2669.
- Johnson B. D., Cooke R. C., 1979, *Bubble populations and spectra in coastal waters: A photographic approach*, J. Geophys. Res., 84, C7, 3761–3766.
- Kolobayev P. A., 1975, *Issledovaniye kontsentratsii i statisticheskogo raspredeleniya razmerov puzyrkov sozdavayemykh vetrom v pripoverkhnostnom sloye okeana*, Okeanologiya, 15, 6, 1013–1017.
- Lovik A., 1980, *Acoustic measurements of the gas bubble spectrum in water*. [In:] *Cavitation and inhomogeneities in underwater acoustics*, Lauterborn W. (Ed), Springer Verlag, Berlin – Heidelberg – New York, 211–218.
- MacIntyre F., 1986, *On reconciling optical and acoustical bubble spectra in the mixed layer*. [In:] *Oceanic Whitecaps*, Monahan E. C., MacNiocaill G. (Eds), Reidel, New York, 75–94.
- Medwin H., 1970, *In situ acoustic measurements of bubble populations in coastal ocean waters*, J. Geophys. Res., 75, 5, 599–611.
- Szczucka J., 1986, *Application of acoustic methods for investigations on inhomogeneities of the Baltic waters*, PhD. Thesis, Institute of Oceanology PAS, Sopot, 157 pp., (in Polish).
- Szczucka J., 1990, *Acoustic detection of gas bubbles in the sea*, Oceanologia, 28, 103–113.